

Simulating long-range hopping with periodically-driven superconducting qubits

Mor M. Roses,¹ Haggai Landa,² and Emanuele G. Dalla Torre¹

¹*Department of Physics and Center for Quantum Entanglement Science and Technology, Bar-Ilan University, 52900 Ramat-Gan, Israel*

²*IBM Quantum, IBM Research Haifa, Haifa University Campus, Mount Carmel, Haifa 31905, Israel*

Quantum computers are a leading platform for the simulation of many-body physics. This task has been recently facilitated by the possibility to program directly the time-dependent pulses sent to the computer. Here, we use this feature to simulate quantum lattice models with long-range hopping. Our approach is based on an exact mapping between periodically driven quantum systems and one-dimensional lattices in the synthetic Floquet direction. By engineering a periodic drive with a power-law spectrum, we simulate a lattice with long-range hopping, whose decay exponent is freely tunable. We propose and realize experimentally two protocols to probe the long tails of the Floquet eigenfunctions and to identify a scaling transition between weak and strong long-range couplings. Our work offers a useful benchmark of pulse engineering and opens the route towards quantum simulations of rich nonequilibrium effects.

A common assumption of many-body physics is that particles can interact only with their neighbors. Similarly, in canonical lattice models, particles are often assumed to hop only between neighboring sites. While generically correct in condensed matter physics, this assumption is not applicable to gravitational models, unscreened Coulomb interactions, and synthetic materials, where the couplings can decay as a power-law. Long-range couplings can lead to counter-intuitive effects, such as violations of thermodynamic identities [1–5] and anomalous mechanisms of information spreading [6–8]. Long-range interactions are further affected by dimensionality [9–11], disorder [12, 13], thermal fluctuations [14, 15], and competing orders [16, 17], giving rise to a wide range of classical and quantum phases with peculiar scaling laws.

The experimental study of these effects requires a simulator where the power-law exponent α is not set by the physical decay of elementary forces and can be tuned continuously. This requirement is partially fulfilled by trapped ions, where phonon-mediated interactions can be used to simulate quantum spin models with power-law decaying couplings, and α can be tuned within a limited range [18, 19]. Here, we propose and realize an alternative approach, based on periodically driven (Floquet) quantum models. In these systems, the frequency components of the wavefunctions give rise to an effective one-dimensional lattice and the harmonics of the drive correspond to arbitrary hopping terms [20]. Intuitively, this synthetic Floquet dimension describes the number of photons absorbed or emitted from the drive. In the theoretical limit of a classical drive, such dimension is infinite in both directions .

To realize our protocol, we use a feature of noisy intermediate-scale quantum (NISQ) computers that has been recently made available via the cloud, namely *pulse engineering*. This term refers to the possibility of feeding arbitrary time-dependent pulses to the device [21–23]. Pulse engineering is commonly used to characterize the

qubits and to optimize the fidelity of a target gate, or of a set of gates [24–36]. Periodic drives have been recently used to create long-range couplings in the physical space [37] and to simulate a two dimensional topological insulator [38]. Here, we use pulse engineering to simulate long-range couplings in the Floquet space.

Floquet theorem [39] guarantees that the time evolution of a system governed by a time-periodic Hamiltonian, $H(t + \tau) = H(t)$, can be written as $|\psi(t)\rangle = \sum_n c_n e^{i\mu_n t} |\phi_n(t)\rangle$. Here, μ_n are the quasienergies, and $|\phi_n(t)\rangle$ are the Floquet functions. These functions are periodic in time, $|\phi_n(t + \tau)\rangle = |\phi_n(t)\rangle$ and can be expanded in a discrete Fourier series,

$$|\phi_n(t)\rangle = \sum_m e^{-im\omega_p t} |\phi_n(m)\rangle, \quad (1)$$

where $\omega_p = 2\pi/\tau$ is the pump frequency. By integrating the Schrödinger equation over one period, one obtains a *time independent* linear system of equations $H_F |\phi_n\rangle = \mu_n |\phi_n\rangle$, where H_F is the Hamiltonian in an enlarged infinite dimensional Floquet space and $|\phi_n\rangle$ is a vector in this space, with $\langle m|\phi_n\rangle = |\phi_n(m)\rangle$. The central block of H_F is given by

$$\begin{pmatrix} H_0 + 2\omega_p & H^{(1)} & H^{(2)} & H^{(3)} & H^{(4)} \\ H^{(-1)} & H_0 + \omega_p & H^{(1)} & H^{(2)} & H^{(3)} \\ H^{(-2)} & H^{(-1)} & H_0 & H^{(1)} & H^{(2)} \\ H^{(-3)} & H^{(-2)} & H^{(-1)} & H_0 - \omega_p & H^{(1)} \\ H^{(-4)} & H^{(-3)} & H^{(-2)} & H^{(-1)} & H_0 - 2\omega_p \end{pmatrix}, \quad (2)$$

where $H^{(m)} = \tau^{-1} \int_0^\tau H(t) e^{im\omega_p t} dt$ is the m^{th} discrete Fourier component of $H(t)$ and we set $\hbar = 1$ [40]. In the limit of large ω_p , the off-diagonal terms of H_F can be treated perturbatively, giving rise to the well-known Magnus expansion. Note that Eq. (1) is invariant under the gauge transformation $|\phi_n(m)\rangle \rightarrow e^{i\omega_p t} |\phi(m+1)\rangle$, and hence H_F is invariant to discrete translations, $m \rightarrow m+1$, $H_F \rightarrow H_F + \omega_p$.

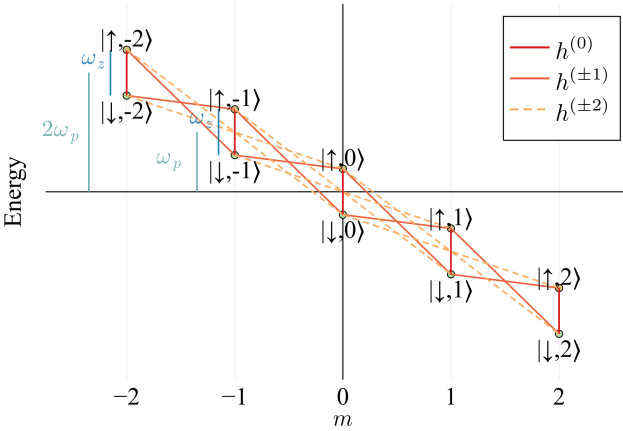


FIG. 1. Schematic plot of the Floquet Hamiltonian for a single qubit described by Eq. (3) with $h(t) = h(t + \tau)$. Each state is characterized by two quantum numbers: spin (\uparrow or \downarrow) and Floquet index (m). The vertical lines show the energy scales: the driving frequency, $\omega_p = 2\pi/\tau$, and the two-level splitting, ω_z . The first and second harmonics of the drive $h^{(\pm 1)}$ and $h^{(\pm 2)}$ correspond, respectively, to nearest neighbour and next-nearest neighbour couplings.

Textbook examples of Floquet systems often involve sinusoidal drives, where $H^{(m)}$ is non zero only for $m = \pm 1$, and H_F corresponds to a tilted lattice with nearest-neighbor couplings. In this case, all the eigenstates of H_F are localized in Floquet space. In analogy to Bloch oscillations of electrons in an electric field, quantum particles oscillate in the Floquet dimension, leading to a periodic alternation of energy emission and absorption (Rabi oscillations). The situation does not change qualitatively when a finite number of harmonics is added. Hence, in most physical situations it is sufficient to focus only on a small segment of the Floquet space [41]. The opposite situation is encountered if the system is periodically driven by delta-functions in time, giving rise to celebrated kicked models [42], where $H^{(m)}$ is independent on m . The Hamiltonian H_F corresponds to a model with all-to-all couplings and its eigenfunctions are completely delocalized in the Floquet space. In this case, a truncation of the Floquet Hamiltonian can lead to unphysical predictions. [43].

Aiming at quantum simulations with superconducting qubits, we specifically consider the spin model

$$H(t) = -\frac{\omega_z}{2}\sigma_z + \frac{h(t)}{2}\sigma_x, \quad (3)$$

where ω_z and $h(t)$ are tunable magnetic fields, and σ_α are Pauli matrices [44]. For $h(t) = h(t + \tau)$ one obtains a Floquet Hamiltonian of the form of Eq. (2), with $H_0 = -\omega_z\sigma_z/2 + h^{(0)}\sigma_x/2$ and $H^{(m)} = h^{(m)}\sigma_x$, where $h^{(m)} = \tau^{-1} \int_0^\tau h(t)e^{im\omega_p t} dt$. This Hamiltonian is equivalent to a two-band Wannier–Stark ladder and is schematically shown in Fig. 1, where, for convenience, we have

depicted $H^{(m)}$ for $|m| \leq 2$ only. To study long-range hopping models, we introduce a time-dependent drive with a power-law frequency spectrum,

$$h^{(m)} = \frac{h_0}{(1 + |m|)^\alpha}. \quad (4)$$

This driving field interpolates between a kicked model at $\alpha = 0$ and a weak sinusoidal drive for $\alpha \gg 1$. At finite α 's, the Fourier transform of Eq. (4) corresponds to periodic kicks with a finite width. The resulting time evolution can be easily computed in two limiting cases: (i) For $\alpha = 0$, the magnetic fields in the x and z directions alternate and the time evolution over one period is $U(\tau) = U_z U_x$ with $U_z = \exp(-i\omega_z \tau \sigma_z/2)$ and $U_x = \exp(-i h_0 \tau \sigma_x/2)$; (ii) For $\omega_z = 0$, the Hamiltonian corresponds to a time-dependent magnetic field in the x direction, whose time evolution is $U(t) = \exp(-i \int dt h(t) \sigma_x/2)$. For finite values of α and ω_z , the Floquet eigenfunctions are evaluated numerically by the diagonalization of the Floquet Hamiltonian in Fig. 2.

We observe that the Floquet functions are composed of a central peak at $m = 0$ and long power-law tails, $|\phi_n(m)\rangle \sim |m|^{-x}$. The value of x can be analytically derived by the following scaling argument: If we consider the product of the m^{th} row of the matrix H_F with the eigenstate, the central peak gets multiplied by $h^{(m)} \sim |m|^{-\alpha}$, while the long tail multiplies the m^{th} diagonal element of H_F , giving rise to a contribution of the order m^{1-x} . Because the eigenvalue does not depend on m , the two contributions needs to scale in the same way and, hence, $x = 1 + \alpha$, or

$$|\phi_n(m)\rangle \sim \frac{1}{|m|^{1+\alpha}}. \quad (5)$$

Note that for all $\alpha \geq 0$, one has $\sum_m |\phi_n(m)|^2 < \infty$, ensuring that the Floquet functions $|\phi_n(t)\rangle$ are normalizable.

In the following, we propose and realize two complementary methods to experimentally probe the power-law tails of the Floquet functions. The first method relies on the relation between the time derivatives of physical observables and the moments of $|\phi_n(m)\rangle$. According to Eq. (1), the q^{th} time derivative of the expectation value of an operator O in the state $|\phi_n(t)\rangle$, $(d/dt)^q \langle O(t) \rangle_n$, equals to

$$(i\omega_p)^q \sum_{m,m'} (m - m')^q \langle \phi_n(m') | O | \phi_n(m) \rangle e^{i(m-m')\omega_p t}.$$

A rigorous bound to this quantity can be obtained by assuming that O satisfies $|\langle \phi_n | O | \phi_m \rangle| \leq \|O\|$, where $\|O\|$ is the operator norm [45]. In this case,

$$\left| \frac{d^q}{dt^q} \langle O(t) \rangle \right| \leq \omega_p^q \|O\| \sum_{m,m'} |m - m'|^q \langle \phi_n(m) | \phi_n(m') \rangle. \quad (6)$$

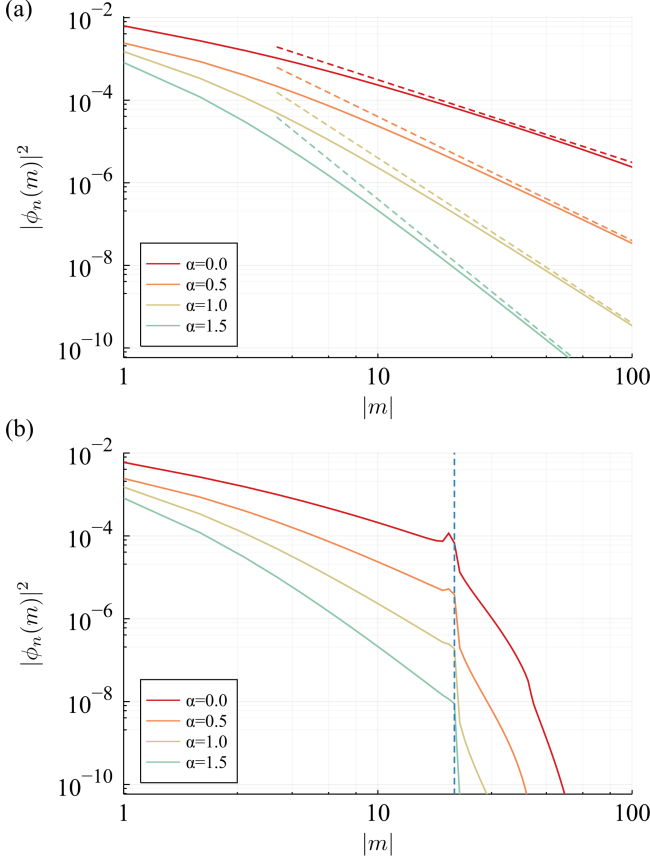


FIG. 2. (a) Eigenstate of the Floquet Hamiltonian: numerical diagonalization of H_F (continuous lines) and power-law asymptotics (dashed lines), Eq. (5). The normalization of the wavefunction is guaranteed by the value of $|\phi_n(m=0)|^2$ (not shown). (b) Numerical diagonalization in the presence of a truncation of the drive at $M = 20$, giving rise to distinctive peak at $m = M$.

Using the scaling relation of Eq. (5), we deduce that the right-hand side of Eq. (6) generically diverges for $q \geq \alpha$. In particular, for the kicked Hamiltonian ($\alpha = 0$) the $q = 0$ series diverges, highlighting the above-mentioned truncation problem. For all $\alpha \leq 1$, the $q = 1$ series diverges, leading to a possible divergence of the time derivative $d/dt \langle O(t) \rangle$. For larger values of α , the $q = 1$ series is convergent, but higher-order series (and, hence, higher order derivatives) are infinite.

In the context of long-range spin models, the point $\alpha = 1$ corresponds to a transition between strong and weak long-range couplings [16, 46]: For $\alpha \leq 1$ the energy is super-extensive and grows faster than the systems size. In our model, this property translates into a divergence of the magnetic field at $t = n\tau$, $h_{\max} = \sum_m h^{(m)}$. To realize this model in a physical system, it is therefore necessary to introduce a truncation parameter. We impose a frequency cutoff, by assuming that $h^{(m)}$ is given by Eq. (4) for all $m \leq M$, and equals 0 for $m > M$. The

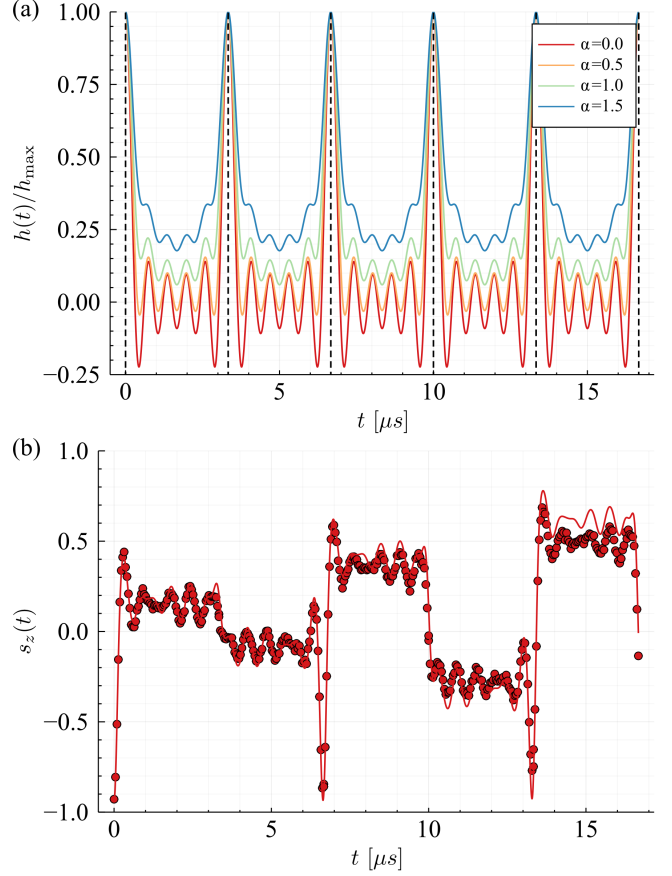


FIG. 3. (a) Time-dependent drive with power law spectrum, Eq. (4), with a truncation at $M = 5$, for different values of α . (b) Time evolution of the qubit for $M = 5$ and $\alpha = 0$, theory (lines) and experiment (dots).

resulting time dependent drive in shown in Fig. 3(a). As we will see, the truncation parameter M offers a powerful knob to probe the power-law tails of the Floquet functions.

Our experimental setup is a single-qubit quantum computer, available on the cloud, the IBM quantum processor Armonk. The typical physical parameters that we use are $\omega_z = 2\pi \times 250$ kHz, $h_{\max} = 2\pi \times 1.2$ MHz, and $\omega_p = 2\pi \times 300$ kHz, or $\tau = 3.3$ μ s. This choice enables us to have $\delta t \ll \tau \ll \min[T_1, T_2]$, where $\delta t = 0.00022$ μ s is the smallest programmable time step and $T_1 = 160$ μ s and $T_2 = 280$ μ s are the decay and coherence times. In our experiment, we prepare the qubit in the $|\downarrow\rangle$ state, set ω_z to a fixed value, apply the drive $h(t)$ for time t , measure the expectation value $s_z(t) = \langle \sigma_z \rangle$ over 8192 shots, and repeat the procedure for 740 time steps between $t = 0$ and $T = 5\tau$, see Fig. 3(b). Figure 4 compares the experimental measurement of the time derivative of $s_z(t)$, with the numerical solution of the time-dependent Schrödinger equation. The scaling behavior changes drastically at the transition between weak and strong long-range couplings ($\alpha = 1$). For $\alpha \leq 1$, $ds_z/dt(t = \tau)$

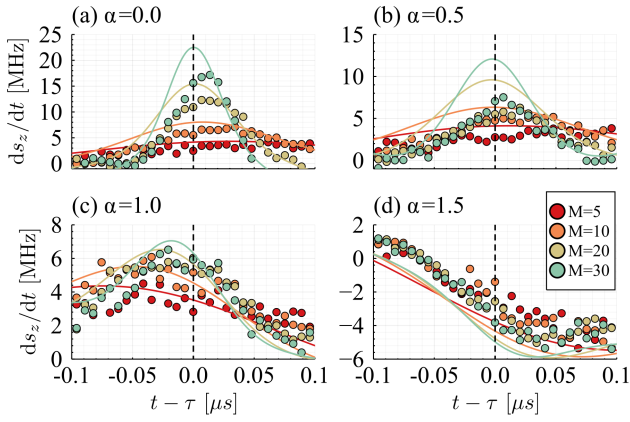


FIG. 4. Time evolution of ds_z/dt in the vicinity of $t = \tau$: theory (lines) and experiment (dots). The truncation parameter M allows us to identify a scaling transition at $\alpha = 1$.

diverges with increasing M , while for $\alpha > 1$ it saturates to a finite value, in agreement with our scaling argument.

Our second method to probe the scaling of the Floquet functions is based on the effects of the truncation on the eigenstates of the enlarged Floquet Hamiltonian H_F . As shown in Fig. 2(b), these functions are unchanged for $m \ll M$, while for $m \gg M$ they decay exponentially. To preserve the normalization condition, the weight lost at $m \gg M$ appears as a pronounced peak at $m \approx M$. The integrated weight of the peak is proportional to $\sum_{m > M} m^{-2-2\alpha} \approx 1/M^{1+2\alpha}$ and rapidly decreases with α . This peak can be experimentally probed by studying the Fourier components $s_z(m) = T^{-1} \int_0^T dt s_z(t) e^{-im\omega_p t}$, see Fig. 5. The key feature that we observe is a pronounced peak at $m = M$. This peak is washed out as α increases and becomes invisible at $\alpha > 1$, probing the scaling transition at $\alpha = 1$.

In conclusion, we used Floquet engineering to simulate a one dimensional lattice with power-law hopping. We studied the scaling properties of the Floquet eigenstates and determined the effects of the long tails on the expectation values of physical observables and their time derivatives. By realizing this model on a quantum computer, we demonstrated the experimental capability of controlling and measuring a large number ($M = 30$) of harmonics. We were able to probe the long tails of the Floquet functions, both in real time and in Fourier space, and to study their dependence on the power-law exponent α . Our experimental observations probe the scaling transition between weak and strong long-range couplings at $\alpha = 1$.

Our work constitutes a significant advancement in the field of quantum simulations with superconducting circuits. This field of research traces back to pioneering experiments on *equilibrium* phase transitions in arrays of Josephson junctions [47–50]. In recent years, superconducting circuits were used to simulate interesting

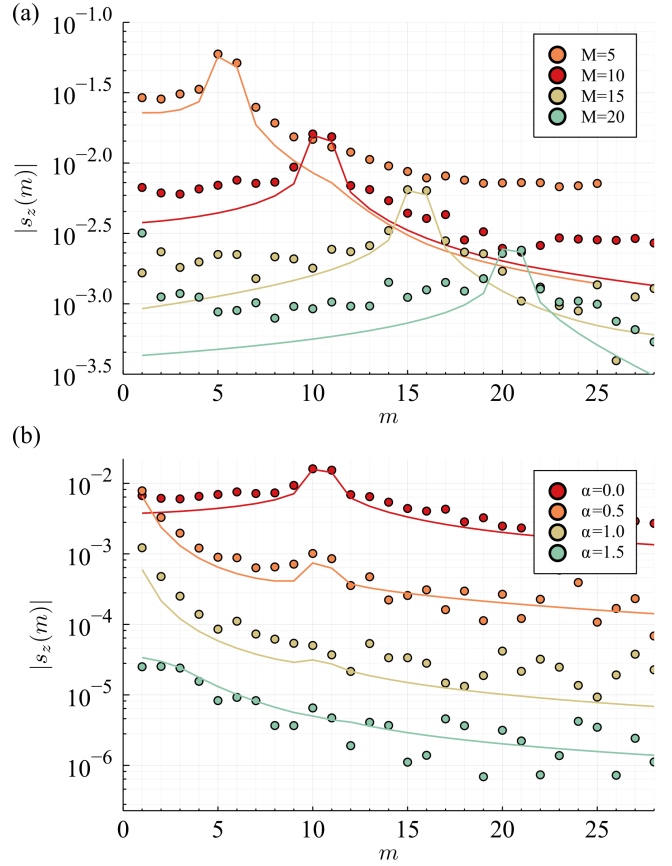


FIG. 5. Amplitude of the discrete Fourier components $s_z(m)$: theory (lines) and experiment (dots). (a) For different values of M at $\alpha = 0$; (b) For different values of α at $M = 10$. The pronounced peak at $m = M$ is an indicator of the long-range nature of the Floquet wavefunction (see text). For clarity, the curves with $\alpha > 0$ in (b) are shifted vertically by $10^{2\alpha}$.

nonequilibrium effects [51, 52], including many-body localization of photons [53] and quench dynamics in one [54] and two [55] dimensions. Our work adds an important tool to these simulators, namely pulse engineering for the realization of synthetic Floquet dimensions. By implementing our protocol on a multi-qubit quantum computer, it will be possible to explore equilibrium and nonequilibrium phase transitions with long-range couplings.

Data availability All MATLAB, Julia, and QISKit codes used to generate the experimental and theoretical data presented in this article are made freely available online in [56].

Acknowledgments We thank Eli Arbel and Angelo Russomanno for useful discussions. We thank the support received through the IBM’s QISKit Slack channels. This work was supported by the Israel Science Foundation grants No. 151/19 and 154/19. The views expressed are those of the authors, and do not reflect the official policy or position of IBM or the IBM Quantum team.

[1] G. Morigi and S. Fishman, Eigenmodes and thermodynamics of a coulomb chain in a harmonic potential, *Physical Review Letters* **93**, 170602 (2004).

[2] F. Bouchet, S. Gupta, and D. Mukamel, Thermodynamics and dynamics of systems with long-range interactions, *Physica A: Statistical Mechanics and its Applications* **389**, 4389 (2010), proceedings of the 12th International Summer School on Fundamental Problems in Statistical Physics.

[3] S. Gupta and S. Ruffo, The world of long-range interactions: A bird's eye view, *International Journal of Modern Physics A* **32**, 1741018 (2017).

[4] A. Campa, T. Dauxois, and S. Ruffo, Statistical mechanics and dynamics of solvable models with long-range interactions, *Physics Reports* **480**, 57 (2009).

[5] A. Campa, T. Dauxois, D. Fanelli, and S. Ruffo, *Physics of long-range interacting systems* (OUP Oxford, 2014).

[6] P. Richerme, Z.-X. Gong, A. Lee, C. Senko, J. Smith, M. Foss-Feig, S. Michalakis, A. V. Gorshkov, and C. Monroe, Non-local propagation of correlations in quantum systems with long-range interactions, *Nature* **511**, 198 (2014).

[7] J. Zhang, G. Pagano, P. W. Hess, A. Kyprianidis, P. Becker, H. Kaplan, A. V. Gorshkov, Z.-X. Gong, and C. Monroe, Observation of a many-body dynamical phase transition with a 53-qubit quantum simulator, *Nature* **551**, 601 (2017).

[8] B. Žunkovič, M. Heyl, M. Knap, and A. Silva, Dynamical quantum phase transitions in spin chains with long-range interactions: Merging different concepts of nonequilibrium criticality, *Physical Review Letters* **120**, 130601 (2018).

[9] F. J. Dyson, Existence of a phase-transition in a one-dimensional ising ferromagnet, *Communications in Mathematical Physics* **12**, 91 (1969).

[10] D. Thouless, Long-range order in one-dimensional ising systems, *Physical Review* **187**, 732 (1969).

[11] J. Sak, Recursion relations and fixed points for ferromagnets with long-range interactions, *Physical Review B* **8**, 281 (1973).

[12] L. Levitov, Critical hamiltonians with long range hopping, *Annalen der Physik* **8**, 697 (1999).

[13] S. Nag and A. Garg, Many-body localization in the presence of long-range interactions and long-range hopping, *Physical Review B* **99**, 224203 (2019).

[14] E. Brezin, G. Parisi, and F. Ricci-Tersenghi, The crossover region between long-range and short-range interactions for the critical exponents, *Journal of Statistical Physics* **157**, 855 (2014).

[15] C. Behan, L. Rastelli, S. Rychkov, and B. Zan, Long-range critical exponents near the short-range crossover, *Physical Review Letters* **118**, 241601 (2017).

[16] A. Campa, G. Gori, V. Hovhannisyan, S. Ruffo, and A. Trombettoni, Ising chains with competing interactions in the presence of long-range couplings, *Journal of Physics A: Mathematical and Theoretical* **52**, 344002 (2019).

[17] B. Xiao, F. Hébert, G. Batrouni, and R. Scalettar, Competition between phase separation and spin density wave or charge density wave order: Role of long-range interactions, *Physical Review B* **99**, 205145 (2019).

[18] D. Porras and J. I. Cirac, Effective quantum spin systems with trapped ions, *Physical Review Letters* **92**, 207901 (2004).

[19] R. Islam, C. Senko, W. Campbell, S. Korenblit, J. Smith, A. Lee, E. Edwards, C.-C. Wang, J. Freericks, and C. Monroe, Emergence and frustration of magnetism with variable-range interactions in a quantum simulator, *Science* **340**, 583 (2013).

[20] See Ref. [57] for an introduction.

[21] A. W. Cross, L. S. Bishop, J. A. Smolin, and J. M. Gambetta, Open quantum assembly language (2017), arXiv:1707.03429 [quant-ph].

[22] D. C. McKay, T. Alexander, L. Bello, M. J. Biercuk, L. Bishop, J. Chen, J. M. Chow, A. D. Córcoles, D. Egger, S. Filipp, J. Gomez, M. Hush, A. Javadi-Abhari, D. Moreda, P. Nation, B. Paulovicks, E. Winston, C. J. Wood, J. Wootton, and J. M. Gambetta, Qiskit backend specifications for openqasm and openpulse experiments (2018), arXiv:1809.03452 [quant-ph].

[23] G. Aleksandrowicz, T. Alexander, P. Barkoutsos, L. Bello, Y. Ben-Haim, D. Bucher, F. Cabrera-Hernández, J. Carballo-Franquis, A. Chen, C. Chen, *et al.*, Qiskit: An open-source framework for quantum computing (2019).

[24] N. Khaneja, T. Reiss, C. Kehlet, T. Schulte-Herbrüggen, and S. J. Glaser, Optimal control of coupled spin dynamics: design of NMR pulse sequences by gradient ascent algorithms, *Journal of magnetic resonance* **172**, 296 (2005).

[25] P. de Fouquieres, S. Schirmer, S. Glaser, and I. Kuprov, Second order gradient ascent pulse engineering, *Journal of Magnetic Resonance* **212**, 412 (2011).

[26] J. Kelly, R. Barends, B. Campbell, Y. Chen, Z. Chen, B. Chiaro, A. Dunsworth, A. G. Fowler, I.-C. Hoi, E. Jeffrey, *et al.*, Optimal quantum control using randomized benchmarking, *Physical Review Letters* **112**, 240504 (2014).

[27] S. J. Glaser, U. Boscain, T. Calarco, C. P. Koch, W. Köckenberger, R. Kosloff, I. Kuprov, B. Luy, S. Schirmer, T. Schulte-Herbrüggen, *et al.*, Training Schrödinger's cat: quantum optimal control, *The European Physical Journal D* **69**, 1 (2015).

[28] D. Lu, K. Li, J. Li, H. Katiyar, A. J. Park, G. Feng, T. Xin, H. Li, G. Long, A. Brodutch, *et al.*, Enhancing quantum control by bootstrapping a quantum processor of 12 qubits, *npj Quantum Information* **3**, 1 (2017).

[29] P. Gokhale, Y. Ding, T. Propson, C. Winkler, N. Leung, Y. Shi, D. I. Schuster, H. Hoffmann, and F. T. Chong, Partial compilation of variational algorithms for noisy intermediate-scale quantum machines, in *Proceedings of the 52nd Annual IEEE/ACM International Symposium on Microarchitecture* (2019) pp. 266–278.

[30] C. Chen, D. Dong, H. Li, J. Chu, and T. Tarn, Fidelity-based probabilistic Q-learning for control of quantum systems, *IEEE Transactions on Neural Networks and Learning Systems* **25**, 920 (2014).

[31] M. Bukov, A. G. Day, D. Sels, P. Weinberg, A. Polkovnikov, and P. Mehta, Reinforcement learning in different phases of quantum control, *Physical Review X* **8**, 031086 (2018).

[32] X.-M. Zhang, Z. Wei, R. Asad, X.-C. Yang, and X. Wang, When does reinforcement learning stand out in quantum control? a comparative study on state preparation, *npj Quantum Information* **5**, 1 (2019).

[33] M. Y. Niu, S. Boixo, V. N. Smelyanskiy, and H. Neven, Universal quantum control through deep reinforcement learning, *npj Quantum Information* **5**, 1 (2019).

[34] J. P. T. Stenger, N. T. Bronn, D. J. Egger, and D. Pekker, Simulating the dynamics of braiding of majorana zero modes using an ibm quantum computer (2020), arXiv:2012.11660 [quant-ph].

[35] T. Alexander, N. Kanazawa, D. J. Egger, L. Capelluto, C. J. Wood, A. Javadi-Abhari, and D. C McKay, Qiskit pulse: programming quantum computers through the cloud with pulses, *Quantum Science and Technology* **5**, 044006 (2020).

[36] S. Garion, N. Kanazawa, H. Landa, D. C. McKay, S. Sheldon, A. W. Cross, and C. J. Wood, Experimental implementation of non-clifford interleaved randomized benchmarking with a controlled-s gate (2020), arXiv:2007.08532 [quant-ph].

[37] V. M. Bastidas, T. Haug, C. Gravel, L. C. Kwek, W. J. Munro, and K. Nemoto, Fully-programmable universal quantum simulator with a one-dimensional quantum processor (2020), arXiv:2009.00823 [quant-ph].

[38] D. Malz and A. Smith, Topological two-dimensional floquet lattice on a single superconducting qubit (2020), arXiv:2012.01459 [quant-ph].

[39] G. Floquet, Sur les équations différentielles linéaires à coefficients périodiques, in *Annales scientifiques de l'École normale supérieure*, Vol. 12 (1883) pp. 47–88.

[40] J. H. Shirley, Solution of the schrödinger equation with a hamiltonian periodic in time, *Physical Review* **138**, B979 (1965).

[41] Remarkably, this approximation remains valid even in situations where the system shows a dynamical instability and the energy absorption rate diverges. For example, the parametric resonance of an harmonic oscillator can be described by considering only two Fourier harmonics [58]. At the resonance, the Floquet functions diverge in Fock space of the oscillator, but remain localized in Floquet space [59].

[42] B. Chirikov and D. Shepelyansky, Chirikov standard map, Scholarpedia **3**, 3550 (2008).

[43] The delocalization of the Floquet eigenfunctions is a necessary condition for the dynamical localization in quantum models of kicked rotors [60, 61].

[44] The Hamiltonian (3) is actually realized in a rotating frame, such that ω_z is the detuning between the driving field and the bare frequency of the qubit, and $h(t)$ is one quadrature of the driving field. We point out that the other quadrature enables one to realize lattice model with imaginary hopping terms.

[45] Pauli matrices are examples of bounded operators with norm $\|O\| = 1$.

[46] N. Defenu, A. Codello, S. Ruffo, and A. Trombettoni, Criticality of spin systems with weak long-range interactions, *Journal of Physics A: Mathematical and Theoretical* **53**, 143001 (2020).

[47] S. Teitel and C. Jayaprakash, Josephson-junction arrays in transverse magnetic fields, *Physical Review Letters* **51**, 1999 (1983).

[48] L. Geerligs, M. Peters, L. De Groot, A. Verbruggen, and J. Mooij, Charging effects and quantum coherence in regular josephson junction arrays, *Physical Review Letters* **63**, 326 (1989).

[49] H. Van der Zant, F. Fritschy, W. Elion, L. Geerligs, and J. Mooij, Field-induced superconductor-to-insulator transitions in josephson-junction arrays, *Physical Review Letters* **69**, 2971 (1992).

[50] H. Van der Zant, W. Elion, L. Geerligs, and J. Mooij, Quantum phase transitions in two dimensions: Experiments in josephson-junction arrays, *Physical Review B* **54**, 10081 (1996).

[51] L. Bassman, M. Urbanek, M. Metcalf, J. Carter, A. F. Kemper, and W. de Jong, Simulating quantum materials with digital quantum computers (2021), arXiv:2101.08836 [quant-ph].

[52] K. Bharti, A. Cervera-Lierta, T. H. Kyaw, T. Haug, S. Alperin-Lea, A. Anand, M. Degroote, H. Heimonen, J. S. Kottmann, T. Menke, W.-K. Mok, S. Sim, L.-C. Kwek, and A. Aspuru-Guzik, Noisy intermediate-scale quantum (nisq) algorithms (2021), arXiv:2101.08448 [quant-ph].

[53] P. Roushan, C. Neill, J. Tangpanitanon, V. M. Bastidas, A. Megrant, R. Barends, Y. Chen, Z. Chen, B. Chiaro, A. Dunsworth, A. Fowler, B. Foxen, M. Giustina, E. Jeffrey, J. Kelly, E. Lucero, J. Mutus, M. Neeley, C. Quintana, D. Sank, A. Vainsencher, J. Wenner, T. White, H. Neven, D. G. Angelakis, and J. Martinis, Spectroscopic signatures of localization with interacting photons in superconducting qubits, *Science* **358**, 1175 (2017).

[54] A. Smith, M. Kim, F. Pollmann, and J. Knolle, Simulating quantum many-body dynamics on a current digital quantum computer, *npj Quantum Information* **5**, 1 (2019).

[55] F. Mei, Q. Guo, Y.-F. Yu, L. Xiao, S.-L. Zhu, and S. Jia, Digital simulation of topological matter on programmable quantum processors, *Physical Review Letters* **125**, 160503 (2020).

[56] M. M. Roses and E. G. Dalla Torre, Simulating long-range hopping with periodically- driven superconducting qubits - data files (2021).

[57] M. S. Rudner and N. H. Lindner, The floquet engineer's handbook (2020), arXiv:2003.08252 [cond-mat.mes-hall].

[58] L. D. Landau and E. M. Lifshitz, *Mechanics: Volume 1*, Vol. 1 (Butterworth-Heinemann, 1976).

[59] S. Weigert, Quantum parametric resonance, *Journal of Physics A: Mathematical and General* **35**, 4169 (2002).

[60] D. Grempel, S. Fishman, and R. Prange, Localization in an incommensurate potential: An exactly solvable model, *Physical Review Letters* **49**, 833 (1982).

[61] S. Fishman, D. Grempel, and R. Prange, Chaos, quantum recurrences, and Anderson localization, *Physical Review Letters* **49**, 509 (1982).